Preprint of paper accepted for publication : https://doi.org/10.1016/j.flowmeasinst.2018.07.003

Non-Invasive Estimation of Domestic Hot Water Usage with Temperature and Vibration Sensors

N.O. Pirow[a], T.M. Louw[b], M.J. Booysen[a,*]

[a] *MTN Mobile Intelligence Lab and Department of E&E Engineering, Stellenbosch University, South Africa*
[b] *Department of Process Engineering, Stellenbosch University, South Africa*

Abstract

Electric water heaters are responsible for a large portion of electricity consumption and water usage in the domestic sector. Smart water heaters alleviate the strain on the electricity supply grid and reduce water consumption through behavioural change, but the installation of in-line flow meters is inconvenient and expensive. A non-invasive water flow meter is proposed as an alternative . Non-invasive flow measurement is more common for high flow rates in the industrial sector than for domestic applications. Various non-invasive water measurement methods are investigated in the context of domestic hot water, and a combination of thermal- and vibration-sensing is proposed. The proposed solution uses inexpensive, easily installable, non-invasive sensors and a novel algorithm to provide the same flow measurement accuracy as existing in-line meters. The algorithm detects the beginning and end of water consumption events with an accuracy of 95.6 %. Quantitative flow rate estimation was possible for flow rates greater than $5\,\mathrm{L\,min^{-1}}$ with an accuracy of 89 %, while volumetric usage estimation had an accuracy of more than 93 %. The algorithm limitations were applied to field data, revealing that water consumption could be detected with an error of less than 12 % within the limitations of the proposed algorithm. The paper presents a successful proof of concept for a non-invasive alternative to domestic hot water flow rate measurement.

Keywords: Hot water flow estimation, smart water heaters, smart grid.

1. Introduction

Water heating with EWHs contributes to 34 % of residential electric energy consumption, which can be reduced with the use of smart EWH controllers (SECs) (de la Rue du Can et al., 2013). Based on known hot water demand patterns, individualised heating schedules and temperature set points can be used by SECs to reduce energy consumption due to water heating without affecting user comfort (Kepplinger et al., 2016; Booysen and Cloete, 2016; Jack et al., 2018; Armstrong et al., 2014). Widespread use of SECs can decrease the strain on the electricity supply grid through peak shaving by implementing demand-side management, which schedules when EWH heating elements can be active, while taking consumer comfort and hot water demand into account (Jack et al., 2018; Roux et al., 2017, 2018). SECs can also decrease the total domestic water consumption by providing users with detailed water consumption feedback. Studies have shown that users who receive consumption feedback decrease their water consumption by adjusting their water usage behaviour (Liu et al., 2017; Ripunda and Booysen, 2018; Fielding et al., 2012b,a).

A limiting aspect of the large-scale deployment of SECs is the non-trivial and expensive plumbing required to install an in-line water flow meter to measure hot water consumption. A non-invasive, retrofit domestic hot water measurement system removes the expensive plumbing associated with SEC installation. This paper addresses this problem by proposing a novel non-invasive flow sensor that uses vibration and temperature sensing to estimate hot water flow through copper piping.

Several non-invasive technologies were investigated in the context of domestic EWH conditions. A combination of vibration and outlet pipe temperature analysis was determined to be the most practical solution. A non-invasive water flow meter for a smart EWH controller was developed using a novel algorithm that requires

*Corresponding author
Email address: mjbooysen@sun.ac.za (M.J. Booysen)

Table 1: Summary of non-invasive water flow rate studies

	Evans et al. (2004)	**Bernier and Brennen (1983)**	**Huijsing et al. (1988)**	**Safari and Tavassoli (2011)**	**Jacobs et al. (2015)**	**Nel et al. (2015)**	**This paper**
Domestic flow rates	✗	✗	✗	✓	✓	✓	✓
Water as working fluid	✓	✓	✗	✓	✓	✓	✓
Low-cost sensing	✓	✗	✓	✓	✓	✓	✓
Copper pipe supported	✓	✗	✓	✓	✗	✓	✓
Robust (noise and location)	✓	✗	✓	✗	✗	✗	✓

temperature and accelerometer data only. The non-invasive flow estimation algorithm was developed using an experimental EWH unit, which was designed to reflect domestic conditions. The selected temperature sensors and accelerometer are inexpensive and readily installed in existing systems, providing an economical retrofit solution.

2. Related Work

Table 1 lists relevant investigations into non-invasive water flow sensors. Non-invasive fluid measurement is common in industrial conditions (Pereira, 2009). Larger pipe diameters and higher fluid flow rates are typically present in industrial conditions than can be expected for domestic EWH conditions. D ata from 34 domestic SEC field units showed maximum measured volumetric flow rates of $30\,\mathrm{L\,min^{-1}}$ (Roux et al., 2017). In contrast, industrial applications discussed by Evans et al. (2004) exhibit flow rates between $500\,\mathrm{L\,min^{-1}}$ and $1500\,\mathrm{L\,min^{-1}}$ for similar pipe diameters. Lower domestic water flow rates often mean that industrial non-invasive flow measurement methods are not suited.

Ultrasonic and electromagnetic methods are commonly employed for the non-invasive measurement of fluid flow. The use of ultrasonic transducers is technically feasible for domestic use (Sanderson and Yeung, 2002), but too expensive for the desired application as components costs alone would exceed current in-line installation method costs. Electromagnetic flow measurement requires an electrically non-conductive inner pipe lining , precluding their use with copper piping (Bernier and Brennen, 1983; Shercliff, 1987).

Thermal methods are generally used to measure gas flow rate (Pereira, 2009). Thermal mass (or thermal dispersion) flow measurement was used by Huijsing et al. (1988) to measure low flow rate liquid flows (below $0.6\,\mathrm{L\,min^{-1}}$) in small diameter pipes (the measuring tube has an inner diameter of 13 mm). Thermal event detection and volumetric estimation were incorporated in an EWH energy usage model by Nel et al. (2015) using a non-invasive temperature sensor installed on the outlet pipe. The data sample rate used was 1 min and the described system was more effective for longer duration flow events (7 to 10 min) and the minimum duration of a detectable usage event was 3 min.

Domestic water flow conditions are almost exclusively turbulent. Rapid velocity fluctuations generated by turbulent flow results in vibrations on the pipe surface, and the magnitude of these vibrations are correlated to the average fluid velocity in the pipe (Evans et al., 2004). An empirically derived quadratic relationship was found between the standard deviation of the vibrations measured using an accelerometer and fluid velocities ranging between $1.82\,\mathrm{m\,s^{-1}}$ and $5.48\,\mathrm{m\,s^{-1}}$ (Evans et al., 2004). These velocities are common in industrial conditions, but greater than that found in domestic applications where the maximum fluid velocity is approximately $0.64\,\mathrm{m\,s^{-1}}$. Another study utilizing condenser microphones to detect vibrations found either linear or quadratic correlations, depending on the sensor position (Safari and Tavassoli, 2011). Time and frequency domain analysis were used to estimate water flow using a piezoelectric transducer installed on a tap outlet, but transitional water flow rates could not be estimated accurately (Jacobs et al., 2015).

From the above information, a combination of vibration and thermal water flow estimation was identified as being the most promising method for low-cost non-invasive flow measurement and were further investigated in the context of domestic EWH conditions.

3. Experimental Unit

3.1. Hardware

A 150 L EWH with a 3 kW heating element and a 600 kPa water supply, as is commonly found in domestic installations, was selected. A diagram of the experimental unit is shown in Fig. 1. A Raspberry Pi 3 was used to sample the sensors, store acquired data, and perform scheduled water usage events for controlled experimental conditions. Water flow rate was controlled using a manually operated ball valve and scheduled water usage (flow events) were controlled by fully opening or closing an electrically operated solenoid valve. Water flow rate was measured using an in-line positive displacement Misol flow meter with a volumetric measurement resolution of 380 pulses per litre and general purpose input/output (GPIO) interrupt handler in software.

Two temperature sensors were mounted on the EWH outlet pipe: one 'near' (T_N) and one 'far' (T_F) a short distance away from the EWH outlet. Inlet pipe (T_{In}) and ambient air (T_∞) sensors were also installed, but were not required for the designed system to function. Texas Instruments TMP275 digital temperature sensors were selected due to their relatively low cost, listed accuracy of $\pm 1\,^\circ$C without calibration, inter-integrated circuit (I^2C) communication, and maximum resolution of 12-bit which equates to 0.0625 °C. Heatsinks were installed on the outlet pipe to maximize the longitudinal temperature difference on the outlet pipe between the upstream and downstream sensors. The heatsinks were milled to have a 22 mm mounting surface to enclose the outlet pipe. This was to provide a 'best case' scenario for thermal investigations. The study indicated that sufficient thermal data was available for the experimental unit that heatsinks and 'far' temperature sensors were not required - but this cannot be confirmed for other installations until field tests are performed. An LSM303 3-axis accelerometer was installed on the inlet pipe, sufficiently far from upstream and downstream disturbances to ensure fully developed turbulent flow was measured.

3.2. Software

A python script was executed on the Raspberry Pi to control the water flow for experiments using the solenoid valve, sample the temperature sensors and accelerometer using I^2C, measure the water flow rate using GPIO pulses, and to store the acquired data in a MySQL database. Data sampling was performed at 1 s intervals. Accelerometer sweeps were performed at $\approx$ 1 kHz and the standard deviation σ of 250 g-force readings per accelerometer axis were stored. The σ values were filtered using a centre-shifted rolling mean (moving average) filter with a window length of 10 s to smooth the signals while maintaining temporal accuracy. Experiments with automated flow events were controlled using the Raspberry Pi and solenoid valve to ensure repeatable conditions.

3.3. Experimental plan

Three separate experiments were performed using the EWH unit to test different aspects of the system. The associated datasets were used to design and test the non-invasive flow estimation algorithm. Table 2 summarises the purposes of each dataset.

Dataset 1 consisted of 5 days of scheduled flow events at a fixed flow rate for each test day. Four clusters or sets of three flow events were executed 6 h apart during each test day. The three flow events which formed

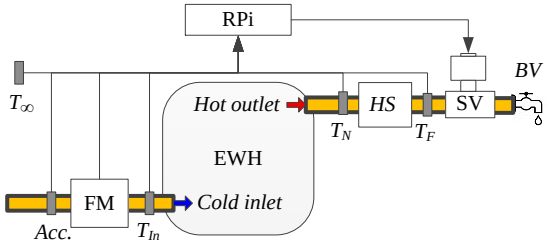

Figure 1: Diagram showing the experimental unit. Outlet pipe temperature sensors (near and far - T_N and T_F respectively), inlet pipe temperature sensor (T_{In}), ambient air temperature sensor (T_∞), heatsinks (HS), electrically operated solenoid valve (SV), manually operated ball valve (BV), flow meter (FM), EWH tank, LSM303 accelerometer and Raspberry Pi (RPi) are shown.

Table 2: Experimental Unit Dataset Summary

Dataset	Purpose	Flow Control
1: Scheduled Flow Events	Design Flow Estimation Algorithm Repeat Testing Minimum Vibration Sampling Requirements	Scheduled
2: Manual Flow Events	Test Instantaneous Flow Rates Test Short Duration Events	Manual
3: Scheduled Cool Down Time	Determine Min Cool Down Time Between Events	Scheduled

each of the daily "test sets" were: a 2 min flow event (followed by 3 min of no flow), another 2 min flow event (followed by 3 min of no flow), and a 5 min flow event. Repeated flow events at fixed flow rates for each day of testing provided sufficient data to design the flow estimation algorithm.

Dataset 2 consisted of manually controlled flow events executed with the intention to test instantaneous flow rate estimation and the effectiveness of the algorithm for shorter flow events.

Dataset 3 consisted of scheduled 1 min flow events with increasing time of no flow between flow events. This was done to determine the minimum cool-down time required between flow events for the algorithm to accurately identify flow events.

4. Flow Estimation Algorithm

The algorithm combines event detection, which provides temporal boundaries of non-invasively detected water flow events, and flow estimation, which provides quantitative volumetric flow estimation values for eligible detected usage events.

4.1. Event Detection

The non-invasive detection of hot water consumption (valid usage events) consisted of two distinct steps. Vibration data was used to flag time-points where the measured vibration standard deviation exceeded empirically determined thresholds, $\sigma > \sigma_{(min)}$. Consecutive flagged samples were grouped together to form "vibration events" which contain the temporal boundaries (start and stop times) of potential usage events.

Some detected vibration events were found to contain no measured water consumption. Thermal event classification used temperature data during flagged vibration events to determine whether water flow or external vibration interference was responsible for each grouped vibration event. Four thermal criteria, TC, were developed. The near temperature (upstream of heatsinks), T_N, and far (downstream of heatsinks), T_F, were used to determine the thermal criteria as shown:

- TC_1: T_N must be above 40 °C at the end of an event.
- TC_2: T_F must be above 35 °C at the end of an event.
- TC_3: Longitudinal temperature difference ($\Delta T = T_N - T_F$) must be below 8 °C at any time during an event.
- TC_4: Time differential of near sensor ($\dot{T}_N$) must have a peak value greater than 0.15 °C/s within 15 s of the start of an event.

If all four thermal criteria were met during a vibration event, then the vibration event was classified as a usage event. Vibration events which did not fulfill all the thermal criteria were classified as interference events.

4.2. Flow Estimation

Once it was determined that a flagged event corresponded to actual hot water consumption, flow rate estimation was performed using the vibration data. An adaptation of the relationship described by Evans et al. (2004) was used to relate vibration standard deviation, σ, to volumetric flow rate, $\dot{V}$ (rather than to fluid velocity as by Evans et al. (2004)). A basic linear approximation between σ and the measured volumetric flow rate, $\dot{V}_M$, was found to provide better results than a basic quadratic approximation for the experimental unit. The dataset is available in the supplementary data in Appendix A.

Accurate tracking of instantaneous flow rates during certain flow events was observed for flow rates $> 5\,\mathrm{L\,min^{-1}}$. Accurate average estimated flow rates for an event with instantaneous flow rate fluctuations indicate that the linear approximation used was sufficient for medium and high flow rates. Low flow rate events ($\leq 5\,\mathrm{L\,min^{-1}}$) were consistently detected with usage event detection as flow events, but quantitative flow rate estimation was found to be unreliable. In the usage event detection phase, it was found that grouped vibration data could be used to determine whether each respective usage event contained flow rates which could reliably be quantitatively estimated. A second set of σ threshold values was established corresponding to the minimum measured σ values for usage events which contained acceptable flow estimation accuracy. Low flow events were thus marked as "unreliable" meaning that quantitative flow estimation would not provide accurate results. Qualitative estimation was investigated for unreliable usage events. Higher flow rate events contribute more to volumetric consumption in the same time span, so estimation errors at low flow rates are likely negligible.

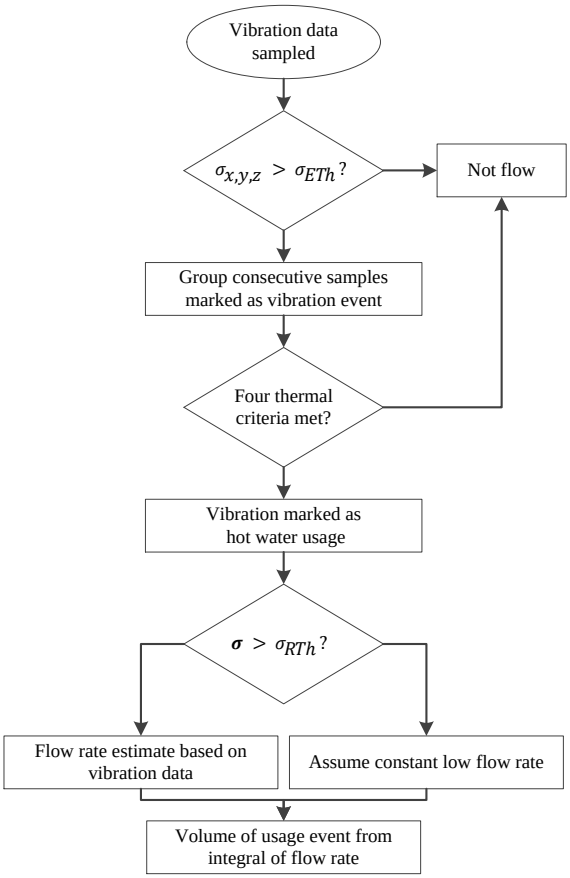

Figure 2: Non-invasive flow rate estimation diagram representing logic used to detect potential flow events using vibration analysis, detection of usage events using thermal analysis, and quantitative flow estimation for events which will yield reliable results based on vibration analysis. σ_{ETh} is the threshold for considering vibration as a potential event. σ_{RTh} is the threshold above which flow rate can be reliably estimated.

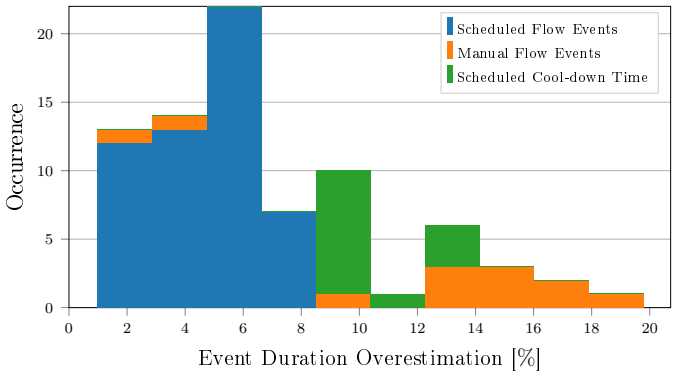

Figure 3: Temporal over-estimation of vibration event detection.

5. Experimental Results

5.1. Limitations

Two algorithm limitations were observed during the design process. The first limitation relates to event detection. Thermal event classification was not successful when insufficient cooldown time, $t_{cd} < 2\,\text{min}$, between flow events was observed. The temperature of the outlet pipe must decrease slightly between flow events for the thermal criteria to be met, otherwise usage events were incorrectly classified as interference events. The second limitation is that quantitative flow rate estimation was only possible for flow rates greater than a minimum value of $\bar{V}_{(min)} \geq 5\,\text{L}\,\text{min}^{-1}$.

5.2. Event Detection

5.2.1. Temporal Boundaries

The non-invasive detection of temporal boundaries of flow events was performed using vibration data. The temporal accuracy of the detected boundaries was assessed by comparing the duration of measured water flow during a vibration event to the non-invasively determined duration of an estimated usage event. It was observed that vibration event detection over-estimated the duration of usage events. It is likely that vibration propagation from the solenoid valve and ball valve contributed to the observed temporal over-estimation. The two flow control valves were situated much closer to the EWH cylinder than the nearest downstream flow control valve in domestic installations.

Fig. 3 shows a histogram of the non-invasive temporal over-estimation of an event as a percentage of the measured duration (using flow meter data). Temporal boundaries were accurate for Scheduled Flow Events, which consisted of flows 2 min and 5 min in duration. Temporal boundaries were less accurate for Manual Flow Events of short duration. Scheduled Cool-down Time events consisted of 1 min duration flow events and consistent temporal over-estimation can be seen for these events (corresponding to the 7 s of solenoid toggle time per event, which is 11 % of the scheduled duration of the flow events).

5.2.2. Usage Event Detection

Thermal event classification was performed for grouped vibration events to non-invasively determine which vibration events were due to hot water flow and which must be disregarded. Table 3 shows the summary of usage event detection in datasets 1 to 3 (Scheduled Flow Events, Manual Flow Events and Scheduled Cool-down Time respectively). The success of using vibration data to identify reliable usage events which can receive quantitative flow rate estimation is also shown.

Fig. 4 shows the measured temperatures of 3 scheduled usage events and TC_1, TC_2 and TC_3. The solid line sections of the measured temperatures show where vibration events occurred, and the dotted sections show where no vibration event was detected. The solid sections thus show the non-invasively determined temporal boundaries of each vibration event wherein thermal event classification takes place.

Fig. 5 shows the fourth thermal criterion used which is that a sufficiently large temperature gradient must be measured for the upstream temperature within 15 s of the start of a vibration event. It was observed that TC_4 was not met when there was insufficient cool-down time between successive water flows. TC_4 was

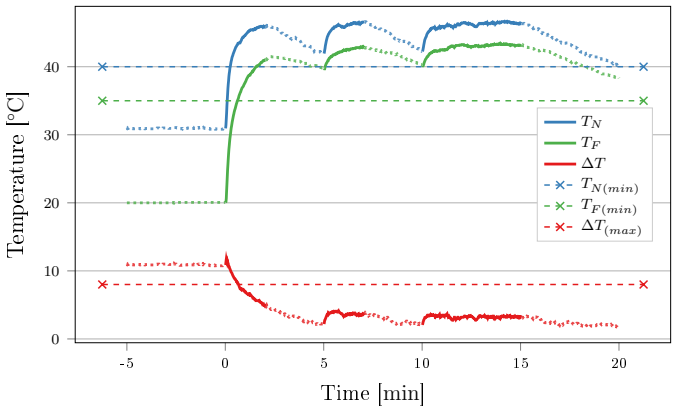

Figure 4: Thermal Criteria 1, 2 and 3 for Event Classification. $TC_1 : T_N \geq 40\,°\text{C}$ (blue), $TC_2 : T_F \geq 35\,°\text{C}$ (green), $TC_3 : \Delta T \leq 8\,°\text{C}$ (red).

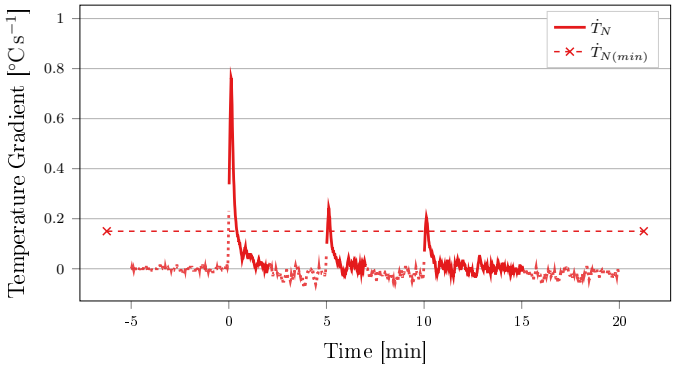

Figure 5: Thermal Criterion 4 Relating to Time Derivative of the Upstream Temperature Sensor. $TC_4 : \dot{T}_N \geq 0.15\,°\text{C}\,\text{s}^{-1}$ within 15 s of event start (red).

Table 3: Experimental unit event detection summary.

Dataset	Usage Events		Reliable Events	
	Expected	Detected	Expected	Detected
1	60	55	45	45
2	12	0	8	8
3	13	6	13	13

however necessary to remove the chance of incorrect classification of external vibration events occurring after valid water flow while the outlet pipe is still warm (which would meet $TC_{1,2,3}$). Strict thermal criteria (which includes TC_4) were used to avoid large consumption overestimations due to vibration interference events.

Table 3 shows that 55 of the 60 scheduled hot water flows were correctly classified as usage events with the remainder occurring during times of external vibration interference. No false positives were found in any dataset but false negatives were observed during external vibration interference in dataset 1 .

The algorithm limitation of a minimum cooldown time, t_{cd}, between events was observed during analysis of dataset 2 (consisting of manually controlled flow events). All flow events in dataset 2 were classified as interference events. Further experiments were performed to determine t_{cd}, using dataset 3 (Scheduled Cool-down Time). Manual classification of vibration events in da tasets 2 and 3 was done to enable more detailed analysis.

The combined effect of the temporal boundary accuracy and the classification of events was assessed by determining what temporal percentage of all measured flow events were valid in dataset 1. Table 4 shows the percentage of duration of all vibration events which were detected during scheduled flow events. Interference

Table 4: Dataset 1 usage event detection summary.

Event Classification	Valid [%]	Invalid [%]
Usage	86.7	3.6
Interference	8.7	1.0
Total	95.4	4.6

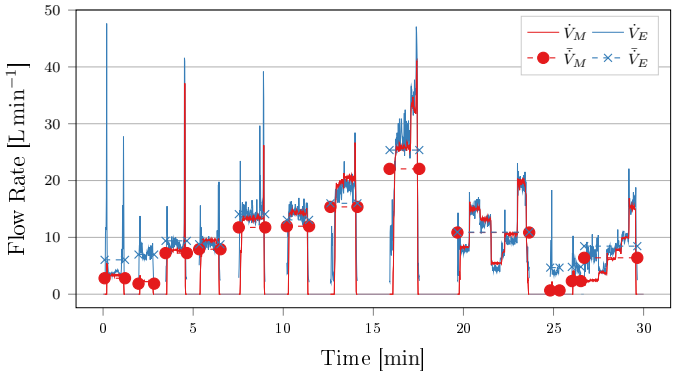

Figure 6: Flow Rate Estimation.

events occurring during flow tests are included. It can be seen that events were correctly classified 95.4 % of the time which shows that usage event detection using non-invasive vibration and temperature data was successful using the algorithm.

5.2.3. Reliable Event Detection

The algorithm is only able to provide reliable quantitative flow rate estimation above $\bar{\dot{V}}_{(min)}$ of 5 L min^{-1}. It was found that the average vibration standard deviation, $\bar{\sigma}$, for grouped events could non-invasively identify events with measured flow rates greater than 5 L min^{-1}. These events were flagged as being 'reliable' and thus eligible for quantitative flow estimation.

Table 3 shows that the identification of reliable usage events was completely successful because all expected reliable usage events were detected. This means that the duration of low flow rate water consumption is known and that a fixed low flow rate approximation can be used for these events. Quantitative flow estimation was performed for reliable usage events.

5.3. Flow Estimation

5.3.1. Instantaneous Flow Rate Estimation

Fig. 6 shows that the estimated flow rate, $\dot{V}_E$, and measured flow rate, $\dot{V}_M$, are similar for instantaneous flow rate changes in dataset 2. The flow events were manually controlled to test a larger variety of flow rates. Large spikes in $\dot{V}_E$ can be seen at the start and ends of usage events, indicating that the manually operated ball valve generated larger vibrations which caused the flow rate overestimation at times.

Instantaneous flow estimation can be seen to be accurate for the usage event starting 20 min into the manually controlled flow events experiment. This event had a long duration (so the vibrations associated with the ball valve did not influence the temporal boundaries as severely as for short events), but contained instantaneous flow rate changes. This indicates that the linear relationship used to estimate flow rates is valid because the algorithm was successful for a wide range of flow rates in a single usage event.

5.3.2. Average Flow Rate Estimation

The average estimated and measured flow rates, $\bar{\dot{V}}_E$ and $\bar{\dot{V}}_M$, are shown in Fig. 6 as dashed lines with end markers. It can be seen that the estimated flow rate is accurate for certain usage events. Usage events with longer durations were more accurately estimated than short events. Dataset 2 also had the greatest

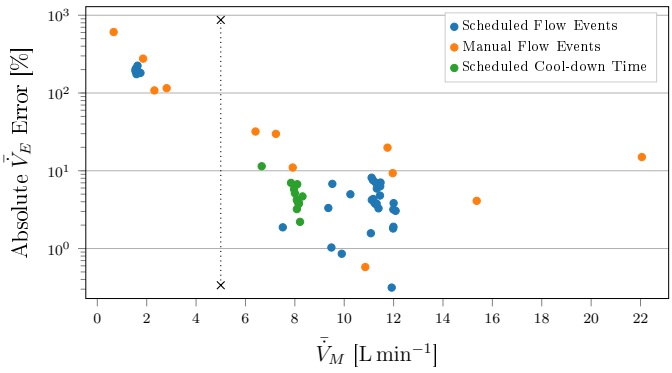

Figure 7: Flow Rate Estimation Error and Flow Rate Scatter Plot.

temporal boundary errors (as shown in Fig. 3) so the manual operation of the ball valve on the outlet pipe was suspected to contribute to the inaccuracy observed.

5.3.3. Estimation Error

Fig. 7 shows the absolute flow rate estimation for all 80 detected usage events in datasets 1 to 3. The vertical line at 5 L min^{-1} shows $\bar{\dot{V}}_{(min)}$ which is the flow rate value to separate qualitative and quantitative flow rate estimation. Low flow rates have an estimation error which is an order of magnitude greater than higher flow rates, which demonstrates the need to determine which detected usage events could be reliably estimated. Higher flow rates have a reasonably consistent estimation accuracy for the flow rates acquired using the experimental EWH unit.

Quantitative flow rate estimation was thus only performed for usage events which were classified as reliable events using vibration data. Fig. 7 shows quantitative flow rate estimation errors for reliable scheduled usage events were below the desired margin of 10 % (with the exception of one Scheduled Flow Event which had an estimation error of −11 %). Estimation errors were greater for manually controlled flow events due to the temporal overestimation associated with vibrations caused by the ball valve.

5.3.4. Volumetric Consumption Estimation

It has been shown that non-invasively determined temporal boundaries of hot water consumption events are accurate, flow rates greater than 5 L min^{-1} can be estimated within the desired accuracy for expected real- world conditions, and usage events can be non-invasively classified to determine if quantitative flow estimation is possible. Fig. 8 shows a histogram of the error between estimated and measured volumetric consumption values for each reliable usage event. The volumetric errors are generally low, especially for datasets 1 and 3 which use the automated solenoid valve to control flow. Table 5 shows the average measured flow rate, total measured consumption, total estimated consumption, and consumption error for the 5 days of scheduled flow events in dataset 1 (external vibration interference are excluded). It can be seen that experimental run 1, with $\bar{\dot{V}}_M$ of 1.63 L min^{-1}, had an unacceptably large estimation error of 195.72 %. All events occurring during experimental run 1 were marked as unreliable by the algorithm. Experimental runs 2 to 5 had mean volumetric estimation errors which are below the desired estimation accuracy of 10 %.

In the above analyses, th measured flow rate, $\dot{V}_M$, and vibrations during detected usage events were analyzed to determine the relationship between flow rate and vibration standard deviation for the experimental unit. A universal relationship cannot be expected for all EWH installations. The piping geometry of each installation affects the vibration propagation so calibration will be required during installation. The desired simplicity of installation and calibration was considered when designing the quantitative flow rate estimation aspect of the algorithm. An example of on- site calibration would be to connect an in-line flow meter to the outlet of a tap and record the flow measurement data for controlled flow events performed by an installation technician. This data can be used to calibrate the non-invasive algorithm for further use.

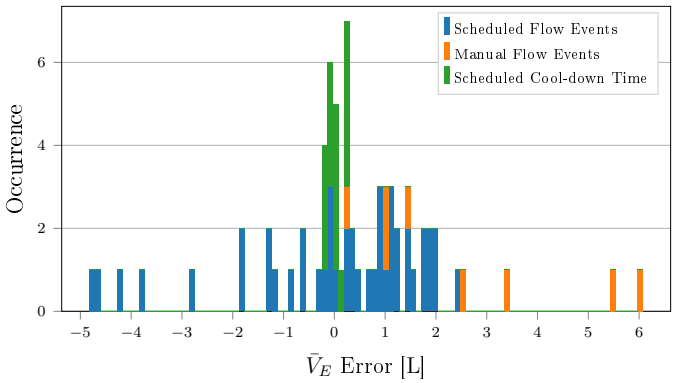

Figure 8: Volumetric Estimation Error for Reliable Usage Events.

Table 5: Dataset 1 volumetric consumption estimation.

Experimental Run	$\bar{\dot{V}}_M$ [L min^{-1}]	$\sum V_M$ [L]	$\sum V_E$ [L]	% Error [%]
1	1.63	47.69	141.02	195.72
2	12.23	446.09	465.82	4.42
3	8.40	306.22	287.03	-6.26
4	10.08	369.19	362.62	-1.78
5	12.13	332.86	338.97	1.83

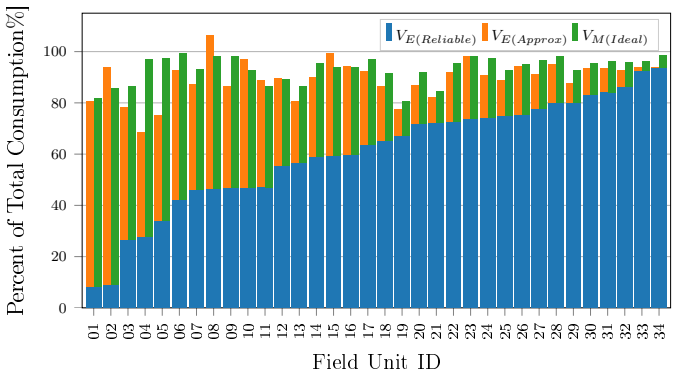

Figure 9: Low Flow Rate Approximation in Field Users Compared to Ideal Measurable Volume.

5.4. Performance of the method on field data

The algorithm is subject to limitations of a minimum cool-down time between flow events ($t_{cd} \geq 2\,\text{min}$) and a minimum flow rate ($\bar{\dot{V}}_{(min)} \geq 5\,\text{L min}^{-1}$) to perform correctly. A field dataset containing the measured water consumption over a period of 4 weeks of 34 anonymous SECs users was acquired. The field dataset was analysed to determine the severity of t_{cd} and $\bar{\dot{V}}_{(min)}$ limitations for real- world usage. This enabled the performance of the designed algorithm to be simulated for real- world conditions.

Fig. 9 shows the percentage of the monthly water consumption which can be estimated using different methods for each user in the field dataset by applying the algorithm limitations to the measured user consumption patterns. The volumetric contribution of events which are more than 2 min apart and contain flow rates greater than $5\,\text{L min}^{-1}$ are shown in blue by $\dot{V}_{E(Reliable)}$. This represents the percentage of each user's consumption which can be reliably estimated when both algorithm limitations are implemented. The estimation value when a constant low-flow approximation is implemented is shown stacked in orange by $\dot{V}_{E(Approx)}$. An approximate low flow value of $2\,\text{L min}^{-1}$ was used (based on the measured flow rate for events less than

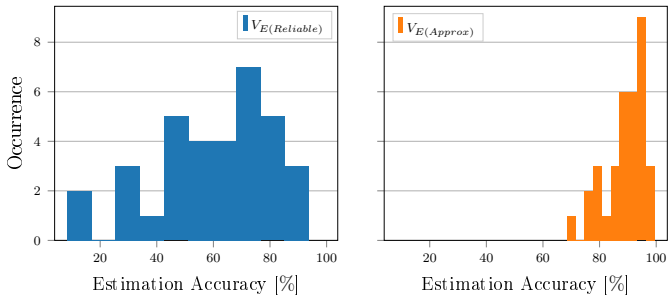

Figure 10: Low Flow Approximation In Field Units to Improve Performance.

Table 6: Low flow approximation and portion of measured consumption which would be estimated.

Method	Percentage of Total Measured consumption [%]						
	Mean	Std	Min	Q1	Q2	Q3	Max
$V_{E(Reliable)}$	60.6	21.9	8.5	46.9	64.4	75.4	93.7
$V_{E(Approx)}$	89.0	6.7	68.5	86.7	90.9	93.6	99.4

$\bar{\dot{V}}_{(min)}$ for the 34 anonymous SEC users). A reference value of the ideal measurable volume, $\dot{V}_{M(Ideal)}$, is shown stacked in green. $\dot{V}_{M(Ideal)}$ is the percentage of volumetric consumption when only t_{cd} limitation is implemented on the dataset (the measured volume during detectable events).

The reliably estimable volumetric consumption for users (blue $\dot{V}_{E(Reliable)}$ bars in Fig. 9) range between 8 % for poorly performing users to 93 % for the best performing user. This is due to user consumption patterns differing. Certain users are therefore very likely to benefit from using the basic non-invasive system while others will not benefit. Without consumption information, it is not possible to determine whether a user is likely to be a good candidate. $\dot{V}_{E(Approx)}$ can be seen to improve user consumption estimations to close to the ideal estimation value, $\dot{V}_{M(Ideal)}$, and improve the performance for all users.

Fig. 10 shows the performance increase when using low-flow approximation for the field dataset. The estimation accuracy, as a percent of the total measured consumption for each user, increases dramatically for poor performing users and additionally benefits better performing users slightly. Table 6 shows the mean, standard deviation, minimum, first quartile, median, third quartile and maximum consumption estimation values. Poorly performing users receive the greatest benefit from low-flow approximation as the minimum value increases from 8.46 % to 68.45 %, and the first quartile increases from 48.89 % to 86.74 %. Low-flow approximation also provides more consistent consumption estimation values for different users (as the standard deviation decreased from 21.92 % to 6.96 %).

6. Conclusion

This paper evaluated the potential of performing non-invasive flow rate estimation for domestic EWH conditions using temperature sensors and an accelerometer.

The designed flow estimation algorithm utilised the combination of vibration and temperature data to non-invasively detect hot water usage events and estimate consumption flow rates and volumes. The algorithm was designed and tested using an experimental EWH unit.

The flow estimation algorithm was limited to a minimum time of 2 min between hot water consumption events for effective usage event detection, as well as a minimum flow rate of 5 L min^{-1} for quantitative non-invasive flow estimation. These limitations were applied to a field dataset containing real world consumption data and the performance was acceptable when low-flow approximation was implemented.

The relatively inexpensive sensors did not require a complex installation procedure which was the intention (to encourage potential users to install a SECs unit).

The proposed solution was proven, but further testing and development is required to determine if the algorithm can be universally successful. Under these conditions, the designed flow estimation algorithm provides an affordable alternative to the existing invasive flow measurement method for the non-invasive

measurement of hot water demand, which can be used to reduce the energy used to heat water in a smart grid with schedule- and temperature-controlling SECs.

7. Acknowledgement

The authors would like to thank MTN for their financial and technical support through the MTN Mobile Intelligence Lab.

References

Armstrong, P., Ager, D., Thompson, I., McCulloch, M., 2014. Improving the energy storage capability of hot water tanks through wall material specification. Energy 78, 128 – 140. URL: http://www.sciencedirect.com/science/article/pii/S0360544214011189, doi:https://doi.org/10.1016/j.energy.2014.09.061.

Bernier, R., Brennen, C., 1983. Use of the electromagnetic flowmeter in a two-phase flow. International Journal of Multiphase Flow 9, 251–257. doi:10.1016/0301-9322(83)90104-0.

Booysen, M.J., Cloete, A.H., 2016. Sustainability through intelligent scheduling of electric water heaters in a smart grid, in: 2016 IEEE 2nd Intl Conf on Big Data Intelligence and Computing (DataCom), pp. 848–855. doi:10.1109/DASC-PICom-DataCom-CyberSciTec.2016.145.

de la Rue du Can, S., Letschert, V.E., Leventis, G., Covary, T., Xia, X., 2013. Energy Efficiency Country Study: Republic of South Africa. Technical Report. Lawrence Berkeley National Laboratory.

Evans, R.P., Blotter, J.D., Stephens, A.G., 2004. Flow Rate Measurements Using Flow-Induced Pipe Vibration. Journal of Fluids Engineering 126, 280. doi:10.1115/1.1667882.

Fielding, K., Spinks, A., Russell, S., Mankad, A., 2012a. Water Demand Management: Interventions to Reduce Household Water Use. Technical Report 94. CSIRO.

Fielding, K., Spinks, A., Russell, S., Mankad, A., 2012b. Water Demand Management Study: Baseline Survey of Household Water Use (Part B). Technical Report 93. CSIRO.

Huijsing, J.H., Dorp, A.L.C.v., Loos, P.J.G., 1988. Thermal mass-flow meter. Journal of Physics E: Scientific Instruments 21, 994–997. doi:10.1088/0022-3735/21/10/017.

Jack, M.W., Suomalainen, K., Dew, J.J.W., Eyers, D., 2018. A minimal simulation of the electricity demand of a domestic hot water cylinder for smart control. Applied Energy 211, 104 – 112. doi:10.1016/j.apenergy.2017.11.044.

Jacobs, H.E., Skibbe, Y., Booysen, M.J., Makwiza, C., 2015. Correlating Sound and Flow Rate at a Tap. Procedia Engineering 119, 864–873. doi:10.1016/j.proeng.2015.08.953.

Kepplinger, P., Huber, G., Petrasch, J., 2016. Field testing of demand side management via autonomous optimal control of a domestic hot water heater. Energy and Buildings 127, 730 – 735. doi:10.1016/j.enbuild.2016.06.021.

Liu, A., Giurco, D., Mukheibir, P., Mohr, S., Watkins, G., White, S., 2017. Online water-use feedback: household user interest, savings and implications. Urban Water Journal 14, 900–907. doi:10.1080/1573062X.2017.1279194.

Nel, P.J.C., Booysen, M.J., v. d. Merwe, B., 2015. Electric water heater energy consumption determination using outlet temperature and volumetric estimation, in: 2015 IEEE Symposium Series on Computational Intelligence, pp. 665–672. doi:10.1109/SSCI.2015.102.

Pereira, M., 2009. Flow meters: Part 1. IEEE Instrumentation & Measurement Magazine 12, 18–26. doi:10.1109/MIM.2009.4762948.

Ripunda, C., Booysen, M.J., 2018. Understanding and affecting water consumer behavior using technological interventions at a primary school in stellenbosch. Water Institute of Southern Africa (WISA) 2018 Conference, South Africa.

Roux, M., Apperley, M., Booysen, M.J., 2018. Comfort, peak load and energy: Centralised control of water heaters for demand-driven prioritisation. Energy for Sustainable Development 44, 78 – 86. doi:10.1016/j.esd.2018.03.006.

Roux, M., Naude, N.H., Booysen, M.J., Barnard, A., 2017. Electric water heaters in smartgrids: Individual savings versus network peak load management, in: SAUPEC 2017, Stellenbosch, Western Cape.

Safari, R., Tavassoli, B., 2011. Initial test and design of a soft sensor for flow estimation using vibration measurements, in: The 2nd International Conference on Control, Instrumentation and Automation, pp. 809–814. doi:10.1109/ICCIAutom.2011.6356765.

Sanderson, M., Yeung, H., 2002. Guidelines for the use of ultrasonic non-invasive metering techniques. Flow Measurement and Instrumentation 13, 125–142. doi:10.1016/S0955-5986(02)00043-2.

Shercliff, J.A., 1987. The theory of electromagnetic flow-measurement. Cambridge science classics, Cambridge University Press, Cambridge New York, NY, USA.

Appendix A. Supplementary material

The dataset used for this study can be found at https://goo.gl/UYSA9u